[5]L. Armstrong, Jr., J. Math. Phys. (to be published).
[6]A. O. Barut and H. Kleinert, Phys. Rev. 156, 1541 (1967); 157, 1180 (1967).
[7]A. O. Barut and C. Fronsdal, Proc. Roy. Soc. (London) A287, 532 (1965).
[8]W. J. Holman III and L. C. Biedenhorn, Jr., Ann. Phys. (N.Y.) 39, 1 (1960); 47, 205 (1968); Kuo-Hsiang Wang, J. Math. Phys. 11, 2077 (1970).
[9]S. Pasternack and R. M. Sternheimer, J. Math. Phys. 3, 1280 (1962).

PHYSICAL REVIEW A VOLUME 3, NUMBER 5 MAY 1971

Correlation Energies and Auger Rates in Atoms with Inner-Shell Vacancies*

Robert L. Chase and Hugh P. Kelly
Department of Physics, University of Virginia, Charlottesville, Virginia 22901

and

H. S. Köhler
Department of Physics, University of Arizona, Tucson, Arizona 85721

(Received 28 December 1970)

Many-body perturbation theory is used to calculate the correlation energy of an atom with an inner-shell vacancy. Numerical calculations are given for neon with either a 1*s* or a 2*s* vacancy. For the case of the 1*s* vacancy, the energy has an imaginary part which is proportional to the Auger rate. Our results are compared with semiempirical determinations of the correlation energy and with experimental results for the fluorescence yield.

I. INTRODUCTION

The many-body perturbation theory of Brueckner[1] and Goldstone[2] is used to calculate the correlation energy of a neon atom in which there is a 1*s* or 2*s* electronic vacancy. The problem is, in principle, the same as that treated by Köhler in calculating nucleon separation energies by K-matrix theory.[3] However, rather than using the spectrum of single-particle states for the N-particle system,[3] we calculate the single-particle states for the $(N-1)$ system in which the vacancy is already present. In the calculations, we use methods discussed previously[4,5] for applying many-body perturbation theory to atoms. We have found it convenient to employ the Silverstone-Yin[6] and Huzinaga-Arnau[7] potential, which has the desirable property that our unexcited states are represented by Hartree-Fock orbitals, while the excited states are calculated in a V^{N-1} potential.[8]

In Sec. II, we discuss the basic theory and considerations in the choice of potential. In Sec. III, we present numerical results for the correlation energy, Auger rates, and fluorescence yield when there is an initial 1*s* vacancy. Numerical results are also presented for the case where there is an initial 2*s* vacancy. Section IV contains the discussion and conclusions.

II. THEORY

A. Singularities in Diagrams

Consider the second-order energy diagram shown in Fig. 1(a). The expression for this diagram is

$$\sum_{k,k'} |\langle kk'|v|pq\rangle|^2 D^{-1} , \tag{1}$$

where

$$D = \epsilon_p + \epsilon_q - \epsilon_k - \epsilon_{k'} . \tag{2}$$

Hole lines p and q refer to unexcited bound states, and k and k' refer to excited single-particle states. The usual two-body interaction is represented by v.

If one of the excited states is a state which normally would have been occupied in the ground state of the atom, the denominator of Eq. (1) may vanish. In this paper, we consider the neon atom with a 1*s* vacancy, and, as a separate case, with a 2*s* vacancy.

In evaluating Eq. (1), sums over bound states are carried out explicitly up to $n=13$, and the n^{-3} rule[8] is used to obtain the contribution from the rest of the bound states. Sums over continuum states are carried out by numerical integration[8] according to

$$\sum_k \rightarrow \frac{2}{\pi}\int_0^\infty dk ,$$

where our continuum states are normalized according to

$$P_{kl}(r) = \cos[kr + \delta_l + (q/k)\ln 2kr - (l+1)\tfrac{1}{2}\pi] , \tag{3}$$

as $r \rightarrow \infty$. The logarithmic term in Eq. (3) arises from the fact that $V(r) \rightarrow q/r$ as $r \rightarrow \infty$.

When excited state $|k\rangle$ is an inner-shell vacancy, D of Eq. (2) may vanish for a particular excited state $|k'\rangle$. In such a case, the singularity in D^{-1} is treated in the usual manner by introducing a

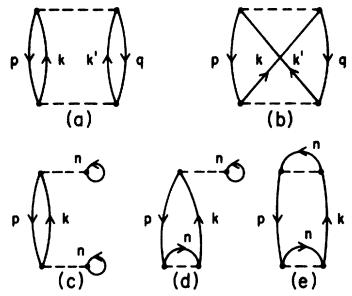

FIG. 1. Second-order energy diagrams. (a) Direct correlation diagram. (b) Exchange. (c)–(e) Single-excitation diagrams. The diagram of (d) with direct and exchange interactions interchanged is also allowed. There are also diagrams like (c)–(e) which contain interactions with the potential V. These single excitation diagrams add to zero when completely unrestricted Hartree-Fock potential is used.

small imaginary part $i\eta$ into D:

$$D \to D + i\eta \tag{4}$$

and

$$(D + i\eta)^{-1} = PD^{-1} - i\pi\delta(D) , \tag{5}$$

where P represents a principal-value integration. We then obtain the following result for Eq. (1) when state $|k\rangle$ is restricted to an excited state which is an inner-shell vacancy:

$$E^{(2)}(p, q) = -2P\sum_{k'} |\langle kk'|v|pq\rangle|^2 [(k' - k_0)(k' + k_0)]^{-1} - (2i/k_0)|\langle kk_0|v|pq\rangle|^2 , \tag{6}$$

where

$$k_0 = [2(\epsilon_p + \epsilon_q - \epsilon_k)]^{1/2} , \tag{7}$$

and state $|k'\rangle$ has an energy of $\frac{1}{2}k'^2$. Atomic units are used throughout this paper. We then obtain a decay rate $4|\langle kk_0|v|pq\rangle|^2/k_0$, corresponding to Auger processes. The excited atomic state may also decay by radiative transitions. The real part of the energy contributes to the correlation energy.

In the higher-order diagrams, we may encounter two or more singularities, and each is treated according to Eqs. (4) and (5).

B. Choice of Potential

In order to carry out perturbation calculations, it is necessary to start with a complete set of single-particle states appropriate to the physical problem. It has been shown that the usual definition of the Hartree-Fock potential, written here in terms of its matrix elements,

$$\langle a|V_{HF}|b\rangle = \sum_{n=1}^{N} (\langle an|v|bn\rangle - \langle an|v|nb\rangle) , \tag{8}$$

is not desirable since excited states are calculated in the field of N electrons rather than $N-1$ other electrons. This difficulty is avoided by the choice of a V^{N-1}-type potential where the sum in Eq. (8) runs from 1 to $N-1$. Further details are given in Ref. 8. The disadvantage of the V^{N-1} potential is that in general, not all single-particle occupied states are Hartree-Fock orbitals, although they are found to be very close.[8,9]

An even better potential has been proposed by Silverstone and Yin,[6] and by Huzinaga and Arnau.[7] In this potential, which we denote by V_{SH}, the occupied orbitals are Hartree-Fock solutions, and the excited states have the desirable property of being calculated in the field of $N-1$ other electrons. Following the notation of Huzinaga and Arnau,[7] the potential may be written

$$V_{SH} = R + (1 - P)\Omega(1 - P) , \tag{9}$$

where R is the Hartree-Fock potential defined in Eq. (8), Ω is an arbitrary Hermitian operator, and P is a projection operator

$$P = \sum_{i=1}^{N} |\phi_i\rangle\langle\phi_i| . \tag{10}$$

It is readily seen that

$$V_{SH}|\phi_i\rangle = R|\phi_i\rangle \tag{11}$$

for $i \leq N$, and that

$$V_{SH}|\phi_j\rangle = (R + \Omega - P\Omega)|\phi_j\rangle \tag{12}$$

for $j > N$. Since all the single-particle states are calculated in the same Hermitian potential, they are orthogonal. The choice of Ω depends on the physical problem under consideration.

Consider the case of the neon atom with an initial $1s$ vacancy. After an Auger transition has taken place, one possible resulting configuration is $(1s)^2(2p)^6ks$, where ks is a continuum state with $l = 0$. The potential V_{SH} may then be used to generate the excited $l = 0$ orbitals in the presence of the $(1s)^2(2p)^6$ core.

The potential R for the $l = 0$ occupied orbitals is

$$R(l = 0) = J^0_{1s} - K^0_{1s} + 2J^0_{2s} - K^0_{2s} + 6J^0_{2p} - K^1_{2p} , \tag{13}$$

where the J^k_{nl} and K^k_{nl} are defined according to their operation on the radial wave function $P_i(r)$:

$$J^k_{nl}P_i(r) = \int_0^\infty dr'(r_<^k/r_>^{k+1})P^*_{nl}(r')P_{nl}(r')P_i(r) , \tag{14}$$

$$K^k_{nl}P_i(r) = \int_0^\infty dr'(r_<^k/r_>^{k+1})P^*_{nl}(r')P_i(r')P_{nl}(r) , \tag{15}$$

where $r_<$ refers to the lesser of r and r', and $r_>$ refers to the greater of r and r'. With R given by Eq. (13), we choose

$$\Omega(l = 0) = J^0_{1s} - (2J^0_{2s} - K^0_{2s}) . \tag{16}$$

We also note that when we use Eq. (13) to solve for the $1s$ state, $J^0_{1s} - K^0_{1s}$ equals zero.

For the $2p$ states, we have

$$R(l=1)=J^0_{1s}-\tfrac{1}{6}K^1_{1s}+2J^0_{2s}-\tfrac{1}{3}K^1_{2s}+5J^0_{2p}-\tfrac{10}{25}K^2_{2p}\ . \quad (17)$$

We choose the Ω for the excited $l=1$ states to be

$$\Omega(l=1)=J^0_{1s}-\tfrac{1}{6}K^1_{1s}-J^0_{2s}+\tfrac{1}{6}K^1_{2s}\ . \quad (18)$$

The excited $l=2$ states may be calculated assuming a post-transition configuration of $(1s)^2(2s)^2(2p)^4kd$. No Ω is needed in this case since the ground state of the neon atom contains no orbitals with $l>1$.

III. NUMERICAL RESULTS

A. Vacancy in 1s Subshell

1. *Calculation Framework*

The ground state of the neon atom with a $1s$ vacancy is a ^2S state, and the unperturbed ground state is a single determinant with orbitals $1s^-$, $2s^\pm$, $2p(\pm1^\pm)$, and $2p(0^\pm)$, where the missing $1s$ orbital has arbitrarily been assigned $m_s=+\frac{1}{2}$. Initially, Hartree-Fock orbitals were calculated using the parameters given by Bagus.[10] These orbitals were then iterated for self-consistency using the potentials of Eq. (13) and (17), in addition to the nuclear attraction. In the self-consistency calculation, the largest difference in the single-particle energies between the last iteration and the previous one was 9×10^{-7}, while the largest difference in the wave functions was 3×10^{-7}.

The excited states were calculated with the potentials

$$V_{SH}|ns\rangle=\{2J^0_{1s}-K^0_{1s}+6J^0_{2p}-K^1_{2p}+|1s\rangle\langle1s|[(2J^0_{2s}-K^0_{2s})-J^0_{1s}]+|2s\rangle\langle2s|[(2J^0_{2s}-K^0_{2s})-J^0_{1s}]\}|ns\rangle \quad \text{for } n>2; \quad (19)$$

$$V_{SH}|np\rangle=\{2J^0_{1s}-\tfrac{1}{3}K^1_{1s}+J^0_{2s}-\tfrac{1}{6}K^1_{2s}+5J^0_{2p}-\tfrac{2}{25}J^2_{2p}-\tfrac{8}{25}K^2_{2p}+|2p\rangle\langle2p|\times[J^0_{2s}-\tfrac{1}{6}K^1_{2s}-J^0_{1s}+\tfrac{1}{6}K^1_{1s}]\}|np\rangle \quad \text{for } n>2; \quad (20)$$

and

$$V_{SH}|nd\rangle=\{2J^0_{1s}-\tfrac{1}{5}K^2_{1s}+2J^0_{2s}-\tfrac{1}{5}K^2_{2s}+4J^0_{2p}-\tfrac{8}{525}J^2_{2p}-\tfrac{32}{225}K^1_{2p}-\tfrac{576}{3675}K^3_{2p}\}|nd\rangle \quad \text{for } n>2. \quad (21)$$

The $\Omega(l=0)$ of Eq. (16) corresponds to calculating the excited $l=0$ states in a $(1s)^2(2p)^6$ core, while the $\Omega(l=1)$ of Eq. (18) corresponds to a $(1s)^2 2s(2p)^5$ core. The choice of $\Omega(l=1)$ is unique since the angular momentum selection rules prevent any other process from yielding an excited $l=1$ orbital.

The bound states were calculated using a computer program similar to that described in Ref. 11, and the continuum states were calculated in a manner described previously.[8] The potential V_{SH} was used in calculating both the bound and the continuum states. All states were orthogonal to better than 10^{-6}.

Completeness tests of the form

$$\sum_k\langle m|1/r|k\rangle\langle k|r|n\rangle-\delta_{mn} \quad (22)$$

were carried out for the sets of single-particle states calculated with the above potentials. Equation (22) was evaluated by summing the bound-state contributions and integrating over the continuum states as previously discussed. Results are given in Table I.

The correlation energy E_{corr} is defined as the difference between the exact nonrelativistic energy and the restricted Hartree-Fock value for the energy. When the Hartree-Fock potential is used, E_{corr} is given by the sum of all second- and higher-order diagrams. In this calculation we determined the *additional* correlation energy introduced by the inner-shell vacancy. For this reason, all many-body diagrams are restricted to the case where one of the particle lines is a vacant inner-shell state. For neon, the denominators of the many-body diagrams may vanish when there is a $1s$ vacancy. When there is a $2s$ vacancy, the denominators do not vanish.

2. *Pair Diagrams*

The lowest-order contributions to both the correlation energy and the Auger rate come from the second-order diagrams shown in Figs. 1(a) and 1(b). Third-order diagrams involving only one pair of excited states p and q are shown in Fig. 2. When we consider the bound excited states, the largest contribution comes from the diagonal interactions, those in which $k''=k$ and $k'''=k'$. Again, state k is restricted to the $1s^+$ state. These diagonal interactions are repeated in higher orders and may be summed geometrically to give the second-order

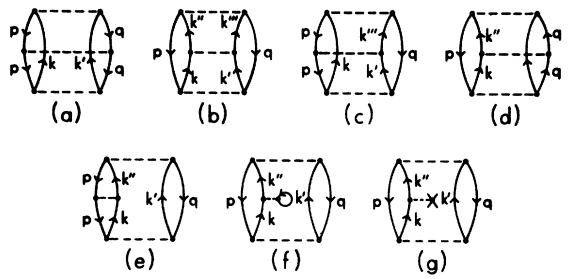

FIG. 2. Third-order contributions to the correlation energy of the pair p,q. Hole-particle interaction in (e) also occurs between states q and k'. Intermediate interaction of (f) and (g) is also included on hole lines p and q and on particle line k'. Exchange diagrams should also be included when states p and q have parallel spin.

term with a shifted denominator[8,12]:

$$E_{\mathrm{corr}}(p,q:k)=\frac{|\langle pq|v|kk'\rangle|^2}{\epsilon_p+\epsilon_q-\epsilon_k-\epsilon_{k'}+\Delta}\ , \tag{23}$$

where we have defined $E_{\mathrm{corr}}(p,q:k)$ as the correlation energy of the pair p,q where one of the excitations is restricted to state k. The quantity Δ is defined as

$$\begin{aligned}\Delta=&-\langle pq|v|(pq)_{ex}\rangle-\langle kk'|v|(kk')_{ex}\rangle+\langle pk'|v|(pk')_{ex}\rangle+\langle qk|v|(qk)_{ex}\rangle\\&-\Big(\sum_{n\neq p}\langle nk|v|(nk)_{ex}\rangle-\langle k|V|k\rangle\Big)-\Big(\sum_{n\neq q}\langle nk'|v|(nk')_{ex}\rangle-\langle k'|V|k'\rangle\Big)\\&+\Big(\sum_{n}\langle np|v|(np)_{ex}\rangle-\langle p|V|p\rangle\Big)+\Big(\sum_{n}\langle nq|v|(nq)_{ex}\rangle-\langle q|V|q\rangle\Big)\ ,\end{aligned} \tag{24}$$

where

$$\langle ab|v|(cd)_{ex}\rangle=\langle ab|v|cd\rangle-\langle ab|v|dc\rangle\ . \tag{25}$$

The potential used to calculate the functions is denoted by V. Since k' is in general a continuum state, diagrams involving interactions with k' were not summed geometrically. The state k is the $1s$ state and thus all other interactions of Fig. 2 may be summed geometrically to give a "modified" second-order result. Inclusion of the correlation energy shift[8,9] into the denominators did not appreciably affect either the real or imaginary parts of the energy.

The second-order "modified" results are shown in Table II. The total result for the pair-correlation energy due to excitations into the vacant $1s$ state is $E_{\mathrm{corr}}(p,q:1s)=-0.00967$ a.u., and the result for the Auger rate is $A_A=0.00897$ atu^{-1} (1 atu $=2.42\times10^{-17}$ sec). The largest contributions to $E_{\mathrm{corr}}(p,q:1s)$ come from the $1s^-$, $2s^+$ and, the $1s^-$, $2p^+$ paris. It is interesting to note that while the $2p(+1^+)$, $2p(+1^-)$ and the $2p(-1^+)$, $2p(-1^-)$ pairs give a small contribution to the correlation energy, they give the largest contribution to the Auger rate. Note that only correlations between $2p$ electrons of opposite spin are shown. This is because diagrams of the type shown in Fig. 1(a) with the $2p$ electrons having parallel spin are exactly cancelled by the exchange diagram of Fig. 1(b).

We must also consider the second-order single excitation diagrams of Figs. 1(c)–1(e). The only difference between our solution and a restricted Hartree-Fock solution is that we have included an additional one-half of an exchange term with the $1s$ electron in both the $2s$ and $2p$ potentials. For this reason only the diagram of Fig. 1(e) contributes, where the state labeled p is either a $2s$ or a $2p$, and state n is the $1s$ state. The state k represents allowed excited states, including the $1s^+$. Figure 1(e) gave a contribution to the correlation energy of -0.00313 a.u. Figure 1(e) does not contribute to the Auger rate.

TABLE I. Completeness tests for single-particle states calculated in the neon core minus one $1s$ electron.[a]

m	n	S[b]
$1s$	$1s$	1.0024
$2s$	$2s$	1.0002
$2s$	$1s$	0.0011
$2p$	$2p$	1.0001

[a] See Eqs. (13) and (17).

[b] $S=\sum_k\langle m|1/r|k\rangle\langle k|r|n\rangle$.

3. *Third- and Higher-Order Diagrams*

The third-order three-body diagrams of Figs. 3(a)–3(e) were also evaluated. There are additional three-body diagrams of the type shown in Fig. 3, but these were calculated or estimated to be small. A complete listing of the third-order three-body diagrams is given in Fig. 4 of Ref. 9. The three-body diagrams were calculated using the previously discussed technique of introducing denominator shifts to sum certain classes of diagrams to all orders. These diagrams gave a result of 0.00067 a.u. for the contribution to the correlation energy, and a 0.00079-atu^{-1} contribution to the Auger rate. The three-body results are given in Table III.

The sum of the two-body and three-body correlation energy terms in which there is an excitation into the $1s^+$ state is then -0.0128 a.u., and the total Auger rate from these terms is 0.00975 atu^{-1}.

The contribution to the Auger rate from the fourth-order diagram of Fig. 3(f) with three imaginary parts was calculated and gave a result of -6×10^{-6} atu^{-1}.

An estimate of the fourth- and higher-order contributions to the correlation energy was made based on a geometric series.[13] This estimate was 10^{-5} a.u. and so was neglected.

4. *Fluorescence Yield*

The fluorescence yield from the K shell ω_K is defined as

$$\omega_K=a_R/(A_R+A_A)\ , \tag{26}$$

where A_A is the Auger rate, and A_R is the radiative rate given by the standard expression for spontaneous emission:

$$A_R = \tfrac{4}{3}(\Delta E/c)^3 |\langle f|\textstyle\sum_i \vec{r}_i|i\rangle|^2 , \quad (27)$$

in atomic units. Since ΔE for our problem is to be the difference between the energies of the atomic state with a $1s$ vacancy and the atomic state with a $2p$ vacancy, we have used the energies for these states calculated by Bagus.[10] Our calculated value for the radiative rate of the $2p$-$1s$ transition in neon is 1.1413×10^{-4} atu^{-1}. This rate was determined by a first-order calculation. We are investigating the effects of correlations on the radiative rate, and preliminary results indicate that these may considerably reduce our calculated radiative rate.

Using our first-order value for the radiative rate we obtain a value for the fluorescence yield of $\omega_K = 0.0143$.

5. *Correlation Energy Relative to* Ne

The quantity of interest in this calculation is $E_{\rm corr}(\mathrm{Ne}^+;\ 1s\ \text{hole}) - E_{\rm corr}(\mathrm{Ne})$, which is defined as the total correlation energy of neon with a $1s$ vacancy minus the total correlation energy of neutral neon. In order to calculate this difference, not only must we calculate the new correlations involving excitations into single-particle states which are occupied in the atom and not in the ion, but also must we include the removal of correlations which were present in the parent atom.

TABLE II. Pair contributions to $E_{\rm corr}(p,q:1s)$ and to the Auger rate in Ne with a $1s$ vacancy.[a]

Electrons[b]	Contribution to $E_{\rm corr}(p,q:1s)$ in a.u.[c]	Auger rate in atu^{-1}
$1s^-, 2s^+$	−0.005 23	0.000 00
$1s^-, 2p^+$	−0.007 58	0.000 00
$2s^+, 2s^-$	−0.000 03	0.000 82
$2s^+, 2p^+$	+0.000 83	0.000 54
$2s^+, 2p^-$	+0.000 19	0.001 65
$2s^-, 2p^+$	−0.000 11	0.000 30
$2p(+1^+), 2p(+1^-)$	+0.000 38	0.001 04
$2p(-1^+), 2p(-1^-)$	+0.000 38	0.001 04
$2p(+1^+), 2p(0^-)$	+0.000 19	0.000 52
$2p(-1^+), 2p(0^-)$	+0.000 19	0.000 52
$2p(+1^+), 2p(-1^-)$	+0.000 13	0.000 32
$2p(-1^+), 2p(+1^-)$	+0.000 13	0.000 32
$2p(0^+), 2p(+1^-)$	+0.000 19	0.000 52
$2p(0^+), 2p(-1^-)$	+0.000 19	0.000 52
$2p(0^+), 2p(0^-)$	+0.000 36	0.000 84
Total	−0.009 66	0.008 97

[a] See Eq. (23).

[b] Terms involving $2p$ states with no m_l designation indicate that each m_l contribution is identical, and the sum is quoted.

[c] Contributions from second-order diagrams in which one of the excited states is the $1s^+$. These results include modified denominators. See Eqs. (23)–(25).

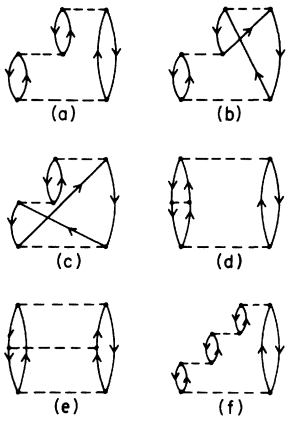

FIG. 3. Higher-order diagrams. Diagrams (a)–(e) are the three-body diagrams included in this calculation. Additional third-order three-body diagrams are discussed in Ref. 9. Diagram (f) is the fourth-order ring diagram.

We must consider the breaking of pair correlations involving the electron which was removed. Using previously reported values of the pair correlations in neon,[14,15] this contribution of pair correlations involving the $1s^+$ electron in the parent atom is calculated to be −0.051 15 a.u.

We have also included the breaking of correlations in the three-body terms. Based on previous estimates of the total three-body contributions to the correlation energy of neon,[14,15] we estimate the three-body correlations in neon involving the $1s^+$ electron to be 0.0062 a.u.

A third contribution to $E_{\rm corr}(\mathrm{Ne}^+;\ 1s\ \text{hole}) - E_{\rm corr}(\mathrm{Ne})$ arises from the fact that the outer electrons in $\mathrm{Ne}^+(1s\ \text{hole})$ feels more of the nuclear charge than do the outer electrons in neutral Ne. This is due to the removal of one of the $1s$ electrons. The magnitude of this effect may be estimated by considering the correlation energy of Na^+ since this also takes into account the action of an additional positive charge on the outer electrons. Using results reported by Clementi,[16] we estimate that this effect adds −0.003 a.u. to the correlation energy of $\mathrm{Ne}^+(1s\ \text{hole})$.

Combining all of the effects which contribute to the difference in correlation energies of $\mathrm{Ne}^+(1s\ \text{hole})$ and neutral Ne, we calculate $E_{\rm corr}(\mathrm{Ne}^+;\ 1s\ \text{hole}) - E_{\rm corr}(\mathrm{Ne}) = 0.029\,82$ a.u. The detailed results are summarized in Table IV.

B. Vacancy in $2s$ Subshell

1. *Potential Choice*

The ground state of the neon atom with a vacancy in the $2s$ subshell is a ^2S state, and the unperturbed ground state is a single determinant with orbitals $1s^\pm$, $2s^-$, $2p(\pm1^\pm)$, and $2p(0^\pm)$. The missing orbital has again arbitrarily been assigned $m_s = +\frac{1}{2}$. The same diagrams used for the case of a $1s$ vacancy were evaluated for the case of a $2s$ vacancy, with the difference that now one of the excited states is restricted to the $2s^+$ state. In the case of the $2s$

TABLE III. Three-body contributions to E_{corr} (Ne^+, 1s hole) and to the Auger rate.

Figure[a]	E_{corr} in a.u.[b]	Auger rate in atu^{-1}
3(a)	0.000725	0.000909
3(b)–3(c)	−0.000133	−0.000247
3(d)	+0.000158	−0.000006
3(e)	−0.000081	0.000133
Total	0.000669	0.000790

[a] Refers to diagrams of Fig. 3.

[b] Contributions from three-body diagrams in which one of the excited states is the $1s^+$.

vacancy, however, the denominators of the correlation energy diagrams do not vanish and so there is no imaginary part to our calculated energies.

In order to improve the accuracy of our calculation we recalculated our 2s and 2p states with the following potentials:

$2s^+$:

$$V = 2J^0_{1s} - K^0_{1s} + J^0_{2s} + 5J^0_{2p} - \tfrac{2}{3}K^1_{2p}\ , \tag{28}$$

$2p$:

$$V = 2J^0_{1s} - \tfrac{1}{3}K^1_{1s} + J^0_{2s} - \tfrac{1}{6}K^1_{2s} + 5J^0_{2p} - \tfrac{10}{25}K^2_{2p}\ . \tag{29}$$

New, low-lying bound excited states with $l=0$ and $l=2$ were calculated in the presence of a $(1s)^2(2s)^2(2p)^4$ core. The rest of the excited states used were those calculated for the case of the 1s vacancy. Various matrix elements were calculated in order to compare results from the case of a 1s vacancy and those from the case of a 2s vacancy. It was found that the above choice of functions was acceptable.

2. *Correlation Energy Relative to* Ne

A "modified" second-order result was obtained by evaluating the diagrams of Figs. 1(a) and 1(b),

TABLE IV. Contributions to $E_{corr}(Ne^+; 1s \text{ hole}) - E_{corr}(Ne)$.

Type of contribution	Value in a.u.
Pair correlations[a]	−0.00967
Three-body correlations[a]	0.00067
One-body corrections[b]	−0.00313
Reduction in shielding[c]	−0.00300
Pair breaking[d]	0.05115
Three-body breaking[d]	−0.00620
Total	0.02982

[a] Terms involving excitations into $1s^+$.

[b] Terms which correct for the difference between our potential and a restricted Hartree-Fock potential.

[c] Energy added due to a reduction in shielding of the nuclear charge introduced by the removal of a 1s electron.

[d] Correlations involving the $1s^+$ electron which were present in Ne and absent in Ne^+ (1s hole).

together with geometrically summed higher-order diagrams of Fig. 2, as explained previously in connection with Eqs. (23) and (24). The correlation energy denominator shifts,[8,9] which did not affect the results for the case of a 1s vacancy, were included here.

The correlation shift Δ_{corr} was evaluated for the case in which both hole lines of Fig. 1(a) were 2p states:

$$\Delta_{corr} = E_{corr}(p, q) + E_{corr}(p, r \neq q) + E_{corr}(r \neq p, q)\ , \tag{30}$$

where $E_{corr}(p, q)$ is the correlation energy of the p-q pair; $E_{corr}(p, r \neq q)$ is the correlation energy of electron p with all unexcited electrons except q; and $E_{corr}(r \neq p, q)$ is the correlation energy of electron q with all unexcited electrons except p. The quantity $\Delta_{corr}(p = 2p,\ q = 2p)$ was evaluated using previously reported pair-correlation energies in neon,[14] and had the value $\Delta_{corr} = -0.1734$ a.u. This correlation shift brought the energy denominators into reasonable agreement with experiment.[17]

The second-order "modified" results are shown in Table V, and had a total value of −0.1019 a.u. The largest pair correlations were those involving 2p electrons. Figure 1(e) was calculated for the state $|n\rangle$, the $2s^+$ state, and gave a value of −0.0034 a.u.

The three-body third-order diagrams of Fig. 3 were evaluated with the denominator shifts previously discussed. These diagrams gave a result of +0.0228 a.u. The detailed results are shown in Table VI.

TABLE V. Second-order contributions to E_{corr} (Ne^+, 2s hole) arising from excitations into the excited $2s^+$ state.

Electrons[a]	Contributions to E_{corr} in a.u.[b]
$1s^+, 1s^-$	−0.00121
$1s^+, 2s^-$	−0.00180
$1s^+, 2p^+$	−0.00215
$1s^+, 2p^-$	−0.00036
$1s^-, 2p^+$	−0.00080
$2s^-, 2p^+$	−0.00645
$2p(+1^+), 2p(+1^-)$	−0.01678
$2p(-1^+), 2p(-1^-)$	−0.01678
$2p(+1^+), 2p(0^-)$	−0.00864
$2p(-1^+), 2p(0^-)$	−0.00864
$2p(+1^+), 2p(-1^-)$	−0.00709
$2p(-1^+), 2p(+1^-)$	−0.00709
$2p(0^+), 2p(+1^-)$	−0.00864
$2p(0^+), 2p(-1^-)$	−0.00864
$2p(0^+), 2p(0^-)$	−0.01278
Total	−0.10195

[a] Terms involving 2p states with no m_l designation indicate that each m_l contribution is identical and the sum is quoted.

[b] Includes modified denominators. See Eqs. (23)–(25).

TABLE VI. Three-body contributions to $E_{corr}(Ne^+;\ 2s\ hole)$.

Figure[a]	Contributions to $E_{corr}(Ne^+;\ 2s\ hole)$ in a.u.[b]
3(a)	0.0427
3(b)–3(c)	−0.0188
3(d)	−0.0006
3(e)	−0.0003
Total	0.0228

[a] Refers to diagrams of Fig. 3.
[b] Contributions from excitations into the $2s^+$ state.

TABLE VII. Contributions to $E_{corr}(Ne^+;\ 2s\ hole) - E_{corr}(Ne)$.

Type of contribution	Value in a.u.
Pair correlations[a]	−0.1019
Three-body correlations[a]	0.0228
Fourth- and higher-order[a]	−0.0042
One-body corrections[b]	−0.0034
Pair breaking[c]	0.4530
Three-body breaking[c]	−0.0050
Total	−0.0464

[a] Terms involving excitations into $2s^+$.
[b] Terms which correct for the difference between our potential and a restricted Hartree-Fock potential.
[c] Correlations involving the $2s^+$ electron which were present in Ne and absent in Ne^+ ($2s$ hole).

An estimate of the fourth and higher-order effects was made via a geometric sum,[13] with the result of −0.0042 a.u.

As in the case of a $1s$ vacancy, certain effects must be calculated in order to obtain a value for $E_{corr}(Ne^+;\ 2s\ hole) - E_{corr}(Ne)$. The breaking of pair correlations involving the $2s^+$ hole state is calculated to be −0.0453 a.u., and the breaking of three-body correlations involving the $2s^+$ state is 0.005 a.u. The reduction in screening of the nuclear charge due to the $2s$ vacancy was estimated to be negligible.

Our total result for $E_{corr}(Ne^+;\ 2s\ hole) - E_{corr}(Ne)$ is then −0.0464 a.u. These results are summarized in Table VII.

IV. DISCUSSION AND CONCLUSIONS

In this calculation, we have used many-body perturbation theory to calculate both the Auger rate and the additional correlation energy introduced in neon when an inner-shell vacancy exists. In order to calculate accurate values for the Auger rate, we calculated the excited single-particle states of the ion with a potential which corresponded to the configuration of the ion after the Auger transition had occurred. This was accomplished through the use of the Silverstone-Yin and Huzinaga-Arnau potential[6,7] which allows us to use restricted Hartree-Fock orbitals for the ground state of the atom yet has the desirable property that the excited states may be calculated with a V^{N-1}-type potential and still remain orthogonal to the ground-state orbitals.

Our results for the additional correlation energy arising from an inner-shell vacancy agree favorably with those reported by Bagus,[10] who used experimental results for the total energy, and performed a restricted Hartree-Fock calculation for the Hartree-Fock energy. We calculate $E_{corr}(Ne^+;\ 1s\ hole) - E_{corr}(Ne) = 0.81$ eV, and $E_{corr}(Ne^+;\ 2s\ hole) - E_{corr}(Ne) = -1.26$ eV, while Bagus quotes 0.65 and −0.84 eV, respectively. The differences in the two separate calculations may partially be attributed to our estimates of the three-body correlation breaking.

A first-order calculation of the fluorescence yield of neon was carried out by McGuire,[18] who used radial wave functions generated with a potential consisting of straight-line approximations to a Herman-Skillman potential. His value for the fluorescence yield, $\omega_K = 0.0185$, is somewhat larger than our value of $\omega_K = 0.0143$. This discrepancy may be entirely attributed to the values used for the radiative rates, since McGuire's value for the Auger rate of 0.00948 atu^{-1} is very nearly the same as our value of 0.00975 atu^{-1}. Our value for the radiative rate for the $2p$-$1s$ transition in neon of 1.413×10^{-4} atu^{-1} is a first-order result, i.e., it includes neither initial-state correlations nor final-state correlations. An investigation of the correlation corrections to the matrix element $\langle 1s|\vec{r}|2p\rangle$ using previously described methods[19] is being carried out. Preliminary results indicated that our value for the radiative rate reported above will be somewhat reduced.

In experimental determinations of the fluorescence yield of neon, Frey *et al.*[20] report a value of $\omega_K = 0.043$, while Heinz[21] reports a value of $\omega_K = 0.018$.

ACKNOWLEDGMENTS

We wish to thank Professor S. Huzinaga and Professor H. Silverstone for kindly sending us reports of their work prior to publication, and to thank Professor C. F. Fischer for several helpful communications. We would like to acknowledge the assistance of Professor A. Batson and his staff at the University of Virginia Computer Science Center, and also several helpful discussions with J. H. Miller.

*Research sponsored in part by the Aerospace Research Laboratories, Office of Aerospace Research, United States Air Force, Contract No. F 33615-69-C-1048.

[1] K. A. Brueckner, Phys. Rev. 97, 1353 (1955).
[2] J. Goldstone, Proc. Roy. Soc. (London) A239, 267

(1957).
[3]H. S. Köhler, Nucl. Phys. 88, 529 (1966).
[4]H. P. Kelly, Phys. Rev. 131, 684 (1963).
[5]H. P. Kelly, Advan. Chem. Phys. 14, 129 (1969).
[6]H. J. Silverstone and M. L. Yin, J. Chem. Phys. 49, 2076 (1968).
[7]S. Huzinaga and C. Arnau, Phys. Rev. A 1, 2285 (1970).
[8]H. P. Kelly, Phys. Rev. 144, 39 (1966).
[9]J. H. Miller and H. P. Kelly, Phys. Rev. A (to be published).
[10]P. S. Bagus, Phys. Rev. 139, A619 (1965).
[11]C. Froese, Can. J. Phys. 41, 1895 (1963), and subsequent revisions.
[12]See especially the discussion on p. 144 of Ref. 5.
[13]H. P. Kelly, Phys. Rev. 173, 142 (1968).
[14]E. R. Davidson and T. L. Barr, Phys. Rev. A 1, 644 (1970).
[15]J. W. Viers, F. E. Harris, and H. F. Schaefer, III, Phys. Rev. A 1, 14 (1970).
[16]E. Clementi, J. Chem. Phys. 39, 175 (1963).
[17]*Atomic Energy Levels*, edited by C. E. Moore, National Bureau of Standards Circular No. 467 (U.S. GPO, Washington, D.C., 1949).
[18]E. J. McGuire, Phys. Rev. 185, 1 (1969).
[19]H. P. Kelly, Phys. Rev. 136, B896 (1964).
[20]W. F. Frey, R. E. Johnston, and J. I. Hopkins, Phys. Rev. 113, 1057 (1959).
[21]J. Heinz, Z. Physik 143, 153 (1955).

PHYSICAL REVIEW A VOLUME 3, NUMBER 5 MAY 1971

Measurement of Lifetime and g Factors by Level Crossing and Optical Double Resonance in the OH and OD Free Radicals

Robert L. deZafra, Alan Marshall, * and Harold Metcalf
State University of New York, Stony Brook, New York 11790
(Received 1 October 1970; revised manuscript received 22 January 1971)

The zero-field level crossing and optical double-resonance techniques have been used to measure the lifetimes and g factors of several rotational substates in the $A^2\Sigma^+$ excited state of the OH and OD free radicals. Optical excitation was provided by a molecular lamp and individual emission transitions were observed through a monochromator in the beam of resonantly scattered light. The measured g factors are in agreement with the results expected from pure case b coupling for this state. The measured lifetimes are 660 ± 22 and 598 ± 20 nsec for OH and OD, respectively; the mean value 629 ± 22 nsec is suggested. The optical double-resonance experiments allow a tentative lower limit to be placed on the excited-state hyperfine interaction.

I. INTRODUCTION

Over the past decade, the Hanle effect (also called the zero-field level-crossing technique)[1] has been used to obtain precision values for lifetimes, g factors, and hyperfine splittings in the electronic excited states of a large variety of atoms. More recently, attention has turned to the extension of this technique, along with the older optical double-resonance (ODR) technique, to obtain molecular parameters and lifetimes of excited molecular states.[2-5] This paper discusses these techniques as we have applied them to a study of the $A^2\Sigma^+$ state of the OH and OD free radicals. Some of the work included here has been previously reported.[3]

From the theoretical point of view, the extension of level crossing to molecular systems is quite straightforward.[4] However, molecules can present rather formidable experimental problems, most of which arise from the rotational and vibrational structure of the electronic states. In particular, because of the rotational structure, single electronic transitions in a typical diatomic molecule give rise to the familiar bands of closely spaced lines, separated by no more than a few tenths of an angstrom, which connect different rotational sublevels between various electronic states. Since the detailed nature of a level-crossing signal depends strongly on the total angular momentum of the initial, excited, and final states, it is necessary to resolve single lines in the band structure in order to fully interpret an experiment. For example, in order to measure the dependence of properties such as g factors on the rotational quantum number of the excited state, it is clearly desirable to isolate single rotational-vibrational transitions.

German and Zare,[5] in experiments similar to ours, surmounted this problem by taking advantage of the fortuitous overlap of an atomic line with one rotational transition in the $A^2\Sigma$-$X^2\Pi$ band of OH. Using the atomic line to excite the molecules, they were able to measure the g factor and lifetime of the $K' = 2$, $J' = \frac{3}{2}$ rotational level of the OH molecule, but this method does not permit a systematic study over rotational levels. In a different approach Isler and Wells[6] used the entire 1-0 band in a CO discharge lamp to provide resonance excitation for a zero-field level-crossing experiment in CO. They attempted to take into account the contributions of the numerous different rotational levels theoretical-